Angewandte
Zuschriften

DOI: 10.1002/ange.201201589

Fuel-Cell Catalysts

Electron Promotion by Surface Functional Groups of Single Wall Carbon Nanotubes to Overlying Metal Particles in a Fuel-Cell Catalyst**

*Patraporn Luksirikul, Karaked Tedsree, Mark G. Moloney, Malcolm L. H. Green, and Shik Chi Edman Tsang**

Noble metals supported on high-surface-area carbon materials are widely used in low-temperature fuel cells.[1] Recent studies have revealed that single-wall carbon nanotubes (SWNTs) with excellent electrical conductivity, high mechanical properties, large surface areas, and well-defined tubular structures should in principle facilitate electron transfer giving better device performance than those of conventional carbon materials.[2,3] However, their tubular shape, consisting of interconnected stable hydrophobic carbon atoms, offers a poor surface to host noble metal particles. As a result, considerable progress has recently been made in the use of functionalized carbon nanotubes in fuel-cell catalysts. For example, oxidation treatment with HNO_3/H_2SO_4 was used to introduce carboxylic acid groups onto the tubular surface to host noble metals.[4,5] Tour and Bahr, and others, demonstrated that aryl diazonium attachment onto carbon nanotubes can provide a uniform derivatized benzene monolayer on a SWNT surface and that these modified materials can be used as fuel-cell supports.[6,7] Their surface affinity, hydrophilicity match, and chelating abilities for the noble metal precursors in solution gives different degrees of metal particle dispersion. Furthermore, these surface organic functional groups are also likely to modify the catalytic performance of the overlying noble metal particles when they are placed in a close proximity.[8] However, there is not yet a systematic study to elucidate such interaction to disentengle this effect from the dispersion.

Herein, we employed a solution-based reduction method by refluxing ethylene glycol/KOH with ammonium tetrachloropalladate to prepare uniform supported Pd nanoparticles of the same size distribution on a range of modified SWNTs with surface organic groups prepared using the Tour method.[9] These supported Pd materials were then studied as anode catalysts in electrocatalytic oxidation of formic acid. Herein, we demonstrate for the first time that the catalytic activity of Pd nanoparticles prepared by this controlled synthesis depends on the type and quantity of surface organic functional groups on the SWNTs. The superior electrocatalytic activity for formic acid oxidation of SWNTs covered with phenolic groups for Pd particles is clearly evident when compared to a commercially available benchmark catalyst and a conventional porous carbon material that has been similarly modified.

The synthesis strategy is summarized in Scheme 1 (for details of the synthesis of Pd nanoparticles deposited onto as-prepared functionalized single-wall carbon nanotubes, f-SWNTs-R, see the Supporting Information). The chemical functionalization of SWNTs with different derivatized aromatic residues (including $C_6H_4CH_2COOH$, $C_6H_4CH_2NH_2$, C_6H_4OH, $C_6H_4NO_2$, and C_6H_4Cl) was achieved according to the solvent-free technique previously reported.[9] These functional-group moieties were selected with various degrees of electron-donating abilities. The success of the chemical attachments was confirmed by Raman, ATR-IR, and TGA (Supporting Information). The different as-prepared f-SWNTs-R were then exploited as supports for Pd in the electrooxidation of formic acid. The Pd size and percentage loading were carefully fixed during the synthesis, giving uniform size and distribution.[10] The XRD patterns (Supporting Information) showed that the supported Pd metal has a face-centered cubic (fcc) structure at the 2θ positions of 40, 46, 67, and 81°, corresponding to (111), (200), (220), and (311) planes. A peak located at 25° is associated with its (002) reflection of SWNTs graphitic plane. The same average Pd size (ca. 5 nm) on all the modified SWNTs-R was derived from the Scherrer's equation.[11] A typical TEM image shown in Figure 1 also indicates that circa 5 nm spherical and uniform Pd particles dispersed on the SWNTs-R with only

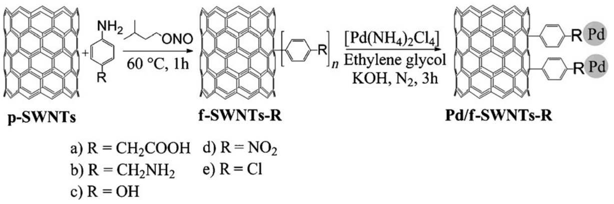

Scheme 1. Preparation of SWNTs with different functional moieties to give f-SWNTs-R. Palladium is then deposited on these as-prepared f-SWNTs-R and p-SWNTs (purified SWNTs). It is assumed that there are no defects on the SWNT surface in this simple model.

---

[*] P. Luksirikul, M. G. Moloney, M. L. H. Green, S. C. E. Tsang
Department of Chemistry, University of Oxford
Oxford, OX1 3QR (UK)
E-mail: edman.tsang@chem.ox.ac.uk

K. Tedsree
Department of Chemistry, Faculty of Science, Burapha University
Chonburi, 20131 (Thailand)

[**] P.L. and K.T. wish to acknowledge the Royal Thai Government for DPhil scholarships to Oxford University.

Supporting information for this article is available on the WWW under http://dx.doi.org/10.1002/anie.201201589.

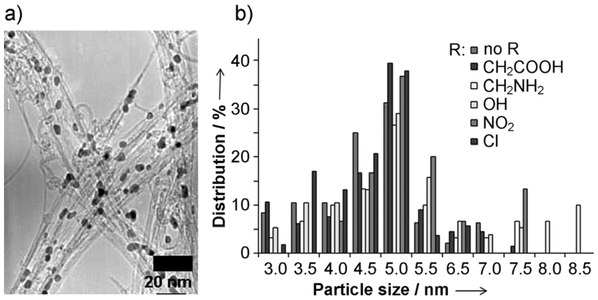

Figure 1. a) A typical TEM image of Pd/f-SWNT-ArCl. b) Histograms showing the same size distribution of Pd nanoparticles (most probable mean size is 5 nm) on different carbon nanotubes supports.

a small degree of particle aggregation. A size histogram from the TEM suggests that the Pd nanoparticle size and distribution on these modified SWNTs were identical within experimental error. The XPS analysis confirmed the presence of Pd^0 on functionalized SWNTs-R. The Raman spectroscopy indicated almost no change in the I_D/I_G relative intensity with the same quantities of tubular defects relative to tubular structure for all of the samples before and after the Pd deposition.

Palladium is known to catalyze formic acid electrooxidation by a direct pathway to produce CO_2 and H_2.[12–15] This electrooxidation reaction was monitored over the Pd on SWNTs with different surface functional groups. A conventional three-compartment cell was therefore used for electrochemical measurements. The working electrode was a glassy carbon film electrode, which was coated with a thin layer of catalyst ink (14 $\mu g\,cm^{-2}$). The electrodes were immersed in 0.5 M H_2SO_4 (electrolyte) and 2.0 M HCOOH (reactant) and the potentials were scanned at a scan rate of 50 $mV\,s^{-1}$ for measurement to obtain the cyclic voltammograms (CV) of circa 5 nm Pd/p-SWNTs and Pd/f-SWNTs-R (Supporting Information). The first scan of the voltammograms and current densities at potential 0.2 V were taken as the arbitrary activities for the comparison of different palladium-SWNT catalysts. Thus, the mass activities (the activity per gram of catalyst) of Pd on different f-SWNTs-R can be summarized (Supporting Information). The mass activity follows the order of f-SWNTs-Cl < f-SWNTs-NO_2 < f-SWNTs-CH_2NH_2 < f-SWNTs-CH_2COOH < f-SWNTs-OH. This order appears to have a correlation with the electron-donating ability of the R group (except that there was leveling off of the mass activities in the cases of hydroxy and carboxylic groups, which is presumably due to attainment of mass limitation over these high-surface-area SWNT materials). Although it would be expected that amine groups would give the highest electron-donating ability to the Pd metal nanoparticles than any of the other functional groups when they are in neutral form,[16] it is evident from this study that the carboxylic acid and phenolic acid moieties gave a higher mass activity than the amine. It should be borne in mind that under the high-pH synthesis, these species will be totally ionized (as phenolate or carboxylate with potassium ions in solid forms, even when placed in acidic solution), and therefore be more strongly electron-donating.

CO stripping voltammetry is another effective method to determine catalytic activity of electrooxidation (pre-adsorbed CO on a given sample, followed by stripping off the CO in H_2O to CO_2 under increasing voltage) in anode fuel cells.[17–19] We attempted to evaluate the electrooxidation activity of CO to CO_2 over our samples in parallel with the CV measurements of formic acid oxidation activity. As a result, CO was allowed to flow through and presaturate the catalyst material for 20 min in 0.5 H_2SO_4, followed by CV stripping for the CO oxidation (Supporting Information). It is interesting to note that an increasing stripping voltage follows the same order, which again reflects the electronic donating ability of these surface groups to the Pd. Interestingly, there is no leveling off for the increasing CO stripping voltage compared to the corresponding mass activities at higher values (Supporting Information), which is due to the fact that CO is pre-adsorbed on palladium nanoparticle surface, which would not encounter diffusion limitation. We dispelled the possibility that the activity differences lead to the variations in the Pd contents because Pd was totally precipitated at the high pH during the synthesis. Furthermore, the exposed metal surface areas of these samples measured using electrochemical surface area by the hydrogen evolution method (ECSA-H) were comparable to each other (Supporting Information). It is thus clear that the electron-donating ability of the R group plays an important effect on the electrochemical activity of the composite material.

Catalytic activity enhancement of metal particles by support materials can be in general attributed to either geometric or electronic effects.[20] For example, a lattice mismatch between the Pd "skin" and the underlying support surfaces may cause an isomorphic (structural) effect on the electronic structure of Pd. The created expansion in lattice parameters of Pd at interface could result in higher activity. We thus checked the lattice constants of different Pd crystalline planes from XRD extensively and found no correlation with respect to the chemical functionalities (Supporting Information).

It would be essential to seek for direct evidence on the electron modification of Pd exerted by the surface pendant groups on the SWNTs. Recently our group has employed solution NMR spectroscopy to probe the ^{13}C nucleus of adsorbed formic acid and formate on unsupported metal catalysts. Despite the fact that a very small degree of chemical shift of the ^{13}C is detected owing to the presence of an oxygen spacer from metal surface (to reduce the Knight shift in a direct contact), this technique can reflect the bonding strengths of these surface species with metal surface.[21,22] In this study, the ^{13}C NMR chemical resonances of $H^{13}COOH$ on Pd/f-SWNTs-R colloids were collected and used to analyze the adsorption strengths of $H^{13}COOH$ at room temperature. The catalysts were dispersed in aqueous $H^{13}COOH$ with a mole ratio of metal nanoparticles to formic acid of 1:1. Polyvinylpyrrolidone (PVP) was added into the sample mixture of Pd supported f-SWNTs-R catalysts and $H^{13}COOH$ to enhance dispersibilities of the catalysts for the NMR analysis. PVP is water-soluble polymer which is generally used to improve the dispersion of carbon nanotubes by non-covalent functionalization[23] and is exploited as a stabilizer for nanoparticle synthesis. To study the effect of concentration of PVP on chemical shift of $H^{13}COOH$ adsorption, the concentration of PVP was varied. It was found that only at a high concentration the PVP can affect the chemical shift value of adsorbed $H^{13}COOH$. As a result, a carefully selected low concentration of PVP was used for all of the samples. Under these conditions with a dilute Pd-containing colloid, the three modes of dissociative formate adsorptions (bridged, multidentate, monodentate) were too weak to be detected.[21] However, a high-intensity signal at 165.37 ppm was clearly detected and assigned to the non-dissociative formic acid adsorption on the metal surface in a rapid exchange with excess free formic acid in solution (a slightly downfield shift compared to the molecular form at 165.76 ppm.[22]). We also observed an NMR signal at 124.55 ppm, which was assigned to free dissolved CO_2.[22] Thus, this result indicates a small degree of decomposition of formic acid to CO_2 and H_2, which represents a direct pathway mechanism for formic acid oxidation even without the input of electrical current.[22] We note that the CO_2 peak gradually increased while formic acid peak steadily decreased along the reaction time, which is strongly indicative of the gradual decomposition of adsorbed formic acid molecule to carbon dioxide and hydrogen. The chemical shift values (with error estimations) over different Pd-supported functionalized SWNTs-R (Figure 2) clearly show an excellent correlation with respect to their order of samples in mass activities (leveling with diffusion limitation) or CO stripping voltage (no diffusion limitation and no leveling off), which in turn depend on electron-donating abilities of the surface functional groups (chemical shift values) in alkaline conditions. It is thus clear that the increase in electron density of the Pd metal surface by the electron-donating groups allows electrons from surface to interact with the π* of the C≡O or related surface bound structure of formic acid or thus strengthening their adsorptions.

To elucidate the effect of surface organic functional groups on supported noble metal nanoparticles is not a straightforward task, as it can be masked by factors such as the variations in material nonhomogeneity, surface coverage, and metal dispersion. However, SWNTs appear to allow such detailed elucidation because of their uniform structure and surface. For efficient utilization of a supported noble metal for fuel-cell applications, it is important to reveal the significant activity promotion effect to Pd exerted by simple organic groups on its surface in this study. However, it is also important to assess the degree of promoting effects of each of the pendant groups to the activity of supported Pd on different carbon materials. A benchmark commercial carbon, Vulcan XC 72R, was used for the comparison. Figure 3 shows the comparison of mass activity for 20% w/w Pd on both Vulcan carbon and SWNTs with and without chemical functionalization. Furthermore, another benchmark commercial catalyst (Johnson Matthey 10% Pd on Vulcan) was included. As seen from the Figure 3, increasing the metal loading from 10% (JM catalyst) to 20% (20% Pd on Vulcan) gives a more than fourfold increase in mass activity, suggesting a high loading is desirable for this reaction. The use of SWNTs clearly outperforms the use of Vulcan with and without surface modifications owing to its higher intrinsic surface area (SA; SA of SWNTs $= 400–900\,m^2g^{-1}$, SA of Vulcan $= 254\,m^2g^{-1}$) and possibly the well-defined tubular structure. It is interesting to note that similar promotion effects for different surface functional groups are also evident and on the same order, showing the generic nature of the promotion, however, to a much lesser extent. Estimations of these organic groups on both the carbon materials by TGA (Supporting Information) suggest that SWNTs-R carry sig-

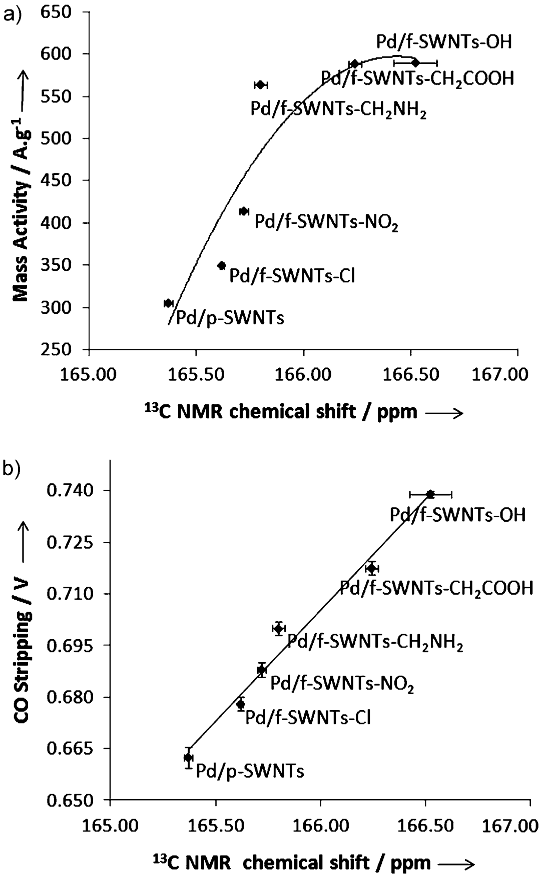

Figure 2. a) A correlation plot between mass activity at a reference voltage of 0.2 V for Pd nanoparticles supported on f-SWNTs-R and their ¹³C NMR chemical shift of adsorbed $H^{13}COOH$, which indicates a diffusion limitation at higher mass activities (leveling off). b) A correlation plot of CO stripping potential and measured chemical shift for all of the Pd samples (no diffusion limitation and no leveling off).

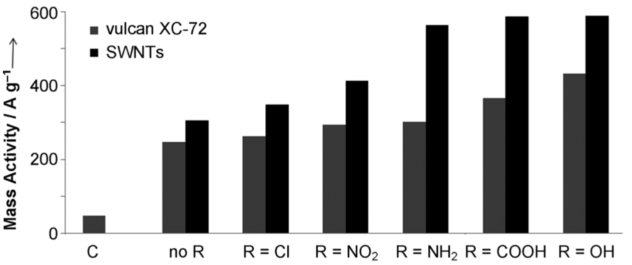

Figure 3. Comparison of mass activity at 0.2 V of commercial 10 w/w% Pd on Vulcan carbon (C), and 20% w/w Pd with both SWNTs and Vulcan carbon with and without chemical modifications (R).

nificantly larger quantities of these groups, which is presumably due to the higher surface area and more well-defined crystalline aromatic tubular surface for the chemical derivatization. Furthermore, the extensive entangling of the small surface-modified nanotubes will also enhance the degree of electronic modification to the overlying Pd particles. Surface phenolate on the SWNTs is apparently the most effective organic group in promoting Pd particles with the same metal content. We estimate that at least 700 $\mathrm{A\,g^{-1}}$ at 0.2 V should be obtained if the diffusion limitation is overcome (Figure 2a and Figure 3). Thus the phenolate groups on SWNTs can enhance the activity of Pd (20 w/w%) more than twofold compared to unmodified SWNTs, and 14 times more than the commercial benchmark Johnson Matthey catalyst (10% w/w on Vulcan).

In conclusion, it has been demonstrated that chemical functionalization of SWNTs can exert a strong electronic promoting effect on the activity of the overlying Pd particles.

Experimental Section

Raw chemical vapor deposition (CVD): SWNTs were supplied by Thomas Swan & Co Ltd. SWNTs were purified using steam treatment at 900 °C for 4 h to remove amorphous carbon and graphitic particles (Supporting Information). The modification of SWNTs were performed using solvent-free technique of different *para*-substituted anilines (Scheme 1): a) 4-acetic acid aniline, b) 4-aminoaniline, c) 4-hydroxyaniline, d) 4-nitroaniline, and e) 4-chloroaniline in isoamyl nitrite to introduce various functional moieties onto tubular walls of SWNTs. Isoamyl nitrite solution (4.8 mol equiv of carbon) was slowly added to the mixture of purified CVD SWNTs (50 mg, 4.167 mmol of carbon) and *para*-substituted anilines (4 mol equiv of carbon) by a syringe in a round-bottom flask. To investigate the electronic effect on Pd, different as-prepared f-SWNTs were exploited as supports for the Pd deposition. A fixed loading of Pd with size control was synthesized by polyol process using ethylene glycol and water mixture as a reducing agent (Supporting Information). In this study, we focused on a 20% w/w loading because it produced Pd/SWNTs that feature high dispersion and short preparation times. The preparation procedure involved the following steps. Pd/SWNTs and Pd/f-SWNTs-R catalysts with 20% w/w metal loading were carried out under basic condition to control their nanoparticle sizes by the added KOH in the precursor solution. Ammonium tetrachloropalladate ($[(NH_4)_2PdCl_4]$, 13.34 mg) was dissolved into ethylene glycol/deionized water (12.50 mL, 1:1 v/v) and then certain amount of KOH (calculated from the stoichiometric concentration) was added into the solution. After the reaction mixture was completely dissolved, purified SWNTs (or as-prepared f-SWNTs-R; 20 mg) were added into the solution. Then, the pH value of the precursor mixture was measured by a pH meter and the pH was adjusted until pH 13.2 was obtained. The reaction precursor was ultrasonicated for 30 min before it was refluxed and stirred for 3 h under N_2 atmosphere in oil bath (170 °C). The reaction product was diluted with deionized water before it was filtered using 0.2 μm polycarbonate membrane then washed thoroughly with deionized water, followed by drying overnight under vacuum at 40 °C. Experimental details (synthesis, testing, and characterization) can be found in the Supporting Information.

Received: February 28, 2012
Revised: April 23, 2012

Keywords: carbon nanotubes · electron transfer · fuel cells · palladium · surface modification

[1] S. E. Habas, H. Lee, V. Radmilovic, G. A. Somorjai, P. Yang, *Nat. Mater.* **2007**, *6*, 692 – 697.
[2] G. Che, B. B. Lakshmi, E. R. Fisher, C. R. Martin, *Nature* **1998**, *393*, 346 – 349.
[3] A. L. Dicks, *J. Power Sources* **2006**, *156*, 128 – 141.
[4] S. C. Tsang, Y. K. Chen, P. J. F. Harris, M. L. H. Green, *Nature* **1994**, *372*, 159 – 162.
[5] S. Banerjee, S. S. Wong, *J. Am. Chem. Soc.* **2003**, *125*, 10342 – 10350.
[6] J. L. Bahr, J. M. Tour, *Chem. Mater.* **2001**, *13*, 3823 – 3824.
[7] J. L. Bahr, J. Yang, D. V. Kosynkin, M. J. Bronikowski, R. E. Smalley, J. M. Tour, *J. Am. Chem. Soc.* **2001**, *123*, 6536 – 6542.
[8] R. Larsen, S. Ha, J. Zakzeski, R. I. Masel, *J. Power Sources* **2006**, *157*, 78 – 84.
[9] C. A. Dyke, J. M. Tour, *Chem. Eur. J.* **2004**, *10*, 812 – 817.
[10] T. Teranishi, M. Hosoe, T. Tanaka, T. Miyake, *J. Phys. Chem. B* **1999**, *103*, 3818 – 3827.
[11] C. C. Murdock, *Phys. Rev.* **1930**, *35*, 8 – 23.
[12] Y. Zhu, S. Y. Ha, R. I. Masel, *J. Power Sources* **2004**, *130*, 8 – 14.
[13] T. Schalow, B. Brandt, D. E. Starr, M. Laurin, S. K. Shaikhutdinov, S. Schauermann, J. Libuda, H. J. Freund, *Phys. Chem. Chem. Phys.* **2007**, *9*, 1347 – 1361.
[14] W. P. Zhou, A. Lewera, R. Larsen, R. I. Masel, P. S. Bagus, A. Wieckowski, *J. Phys. Chem. B* **2006**, *110*, 13393 – 13398.
[15] W. J. Zhou, J. Y. Lee, *J. Phys. Chem. C* **2008**, *112*, 3789 – 3793.
[16] M. Vanden Brink, M. A. Peck, K. L. More, J. D. Hoefelmeyer, *J. Phys. Chem. C* **2008**, *112*, 12122 – 12126.
[17] P. Waszczuk, T. M. Barnard, C. Rice, R. I. Masel, A. Wieckowski, *Electrochem. Commun.* **2002**, *4*, 599 – 603.
[18] T. J. Schmidt, H. A. Gasteiger, B. D. Stab, P. M. Urban, D. M. Kolb, E. J. Behm, *J. Electrochem. Soc.* **1998**, *145*, 2354 – 2358.
[19] H. A. Gasteiger, N. Markovic, P. N. Ross, E. J. Cairns, *J. Phys. Chem.* **1994**, *98*, 617 – 625.
[20] V. R. Stamenkovic, B. Fowler, B. S. Mun, G. F. Wang, P. N. Ross, C. A. Lucas, N. M. Markovic, *Science* **2007**, *315*, 493 – 497.
[21] K. Tedsree, A. T. S. Kong, S. C. Tsang, *Angew. Chem.* **2009**, *121*, 1471 – 1474; *Angew. Chem. Int. Ed.* **2009**, *48*, 1443 – 1446.
[22] K. Tedsree, C. W. A. Chan, S. Jones, Q. Cuan, W.-K. Li, X.-Q. Gong, S. C. E. Tsang, *Science* **2011**, *332*, 224 – 228.
[23] M. J. O’Connell, P. Boul, L. M. Ericson, C. Huffman, Y. Wang, E. Haroz, C. Kuper, J. Tour, K. D. Ausman, R. E. Smalley, *Chem. Phys. Lett.* **2001**, *342*, 265 – 271.